

The formation of the Kuiper belt by the outward transport of bodies during Neptune's migration

Harold F. Levison^{1,2} & Alessandro Morbidelli²

¹Southwest Research Institute, Boulder, Colorado 80302, USA

²Observatoire de la Côte d'Azur, 06304 Nice Cedex 4, France

The 'dynamically cold Kuiper belt' consists of objects on low-inclination orbits between ~40 and ~50 AU from the Sun. It currently contains material totalling less than a tenth the mass of the Earth^{1,2}, which is surprisingly low because, according to accretion models^{3,4}, the objects would not have grown to their present size unless the cold Kuiper belt originally contained tens of Earth masses of solids. Although several mechanisms have been proposed to produce the observed mass depletion, they all have significant limitations⁵. Here we show that the objects currently observed in the dynamically cold Kuiper belt were most probably formed within ~35 AU and were subsequently pushed outward by Neptune's 1:2 mean motion resonance during its final phase of migration. Combining our mechanism with previous work^{6,7}, we conclude that the entire Kuiper belt formed closer to the Sun and was transported outward during the final stages of planet formation.

Since the discovery of the first Kuiper-belt object ten years ago⁸, a picture has emerged that shows a Kuiper belt with two major components: a dynamically cold population—made of objects on orbits with inclinations $i < 4^\circ$ —and a hot population—made of objects whose inclinations can be as large as 30° , and possibly larger⁹. These populations have different physical properties^{10,11}. In addition, there is a small population (roughly 10% of the total) of objects trapped in mean motion resonances (MMRs) with Neptune. The objects in all three structures have semi-major axes less than ~50 AU (refs 12, 13), at which point the Kuiper belt seems to end abruptly (see Fig. 1a).

A study of the literature suggests the following for the early evolution of the Kuiper belt. First, the proto-planetary disk was truncated at roughly 50 AU by one of several possible mechanisms^{14–17}. Then, the dynamical evolution of objects during Neptune's outward migration^{7,18} gave rise to the resonant populations^{6,7}, the hot population^{6,19}, and a related structure known as the scattered disk^{20,21}. This would imply that the objects in the cold population are primordial, presenting us with the mass depletion problem mentioned above.

Here we argue that the initial proto-planetary disk was truncated somewhere near the current location of Neptune (at 30 AU). Placing the edge of the disk at this location provides a natural explanation for why Neptune is where it is—it migrated until it hit the edge of the disk²². Not only the hot population⁶ but also the cold population formed interior to this edge, and was pushed out to its current position during Neptune's migration. This circumvents the mass depletion problem because the mass required for the objects to grow was never in the Kuiper belt. However, the push-out mechanism for the cold population must be different from (but work in conjunction with) that proposed⁶ for the origin of the hot population. This is because that model⁶ involves objects that were scattered by Neptune and thus had their inclinations excited, whereas the inclinations of objects in the cold belt are small. We present a new dynamical mechanism that meets this constraint.

We started our search for a new push-out mechanism by focusing on Neptune's 1:2 MMR. The visible outer edge of the cold belt is close to this MMR's current location at 48 AU (Fig. 1a), which suggested that this resonance might be responsible for this population.

Previous studies⁷ have shown that as Neptune migrated outward, some objects in primordial, low-inclination, low-eccentricity orbits were trapped in this MMR and were pushed outward, along with the resonance. In addition, it was shown that 1:2 MMR does not excite inclinations. Thus, we reasoned that this resonance could have been responsible for the delivery of objects to the region between 40 and 48 AU while keeping the population dynamically cold. However, the standard 'adiabatic model' of resonance trapping predicts that, as the bodies are pushed outwards, their eccentricities monotonically increase. So, as the MMR is pushed through the cold belt, the eccentricities of trapped objects would be larger than those of the observed cold Kuiper-belt objects (see legend of Fig. 1b for details).

But does the adiabatic theory apply to this case? To answer this question, we have simulated, using direct N -body techniques, the evolution of a system containing the four giant planets embedded in a planetesimal disk. The disk extended originally from 10 to 35 AU and contained 50 Earth masses, with a surface density proportional to the inverse heliocentric distance. The disk was modelled using 15,634 particles of equal mass, which interacted with the planets but not with each other, as is usually done in this kind of simulation. The initial locations of Jupiter, Saturn, Uranus and Neptune were at 5.4, 8.7, 13.8 and 18.1 AU respectively. We followed the evolution of this system with the symplectic integrator known as SyMBA^{23,24}. We found that during the integration, the giant planets migrated, owing to the interaction with the disk particles, as expected. In addition,

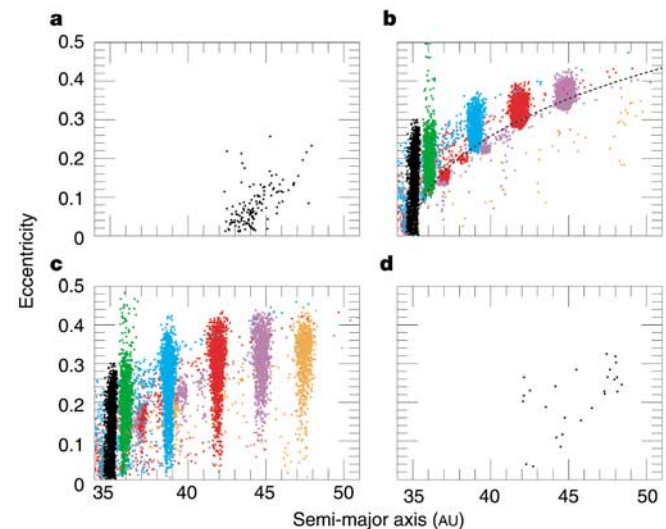


Figure 1 The semi-major axis versus eccentricity distribution for various 'cold' populations. In all cases only objects with inclinations less than 4° are plotted. **a**, Real Kuiper-belt objects. Only those objects that have been observed over multiple oppositions are plotted, to ensure accurate orbits. **b**, Migration if the resonant particles (but not other particles if they are present) are massless. The colours represent different times and thus the 1:2 MMR was at different locations: 6 Myr (black), 8 Myr (green), 16 Myr (blue), 25 Myr (red), 38 Myr (purple) and 98 Myr (orange). At these times, Neptune was at approximately 22 AU, 24 AU, 26 AU, 28 AU and 30 AU, respectively. The black and green data were taken from our direct N -body simulation while the rest were taken from our 'smooth migration' runs. Secondary clumps of a given colour are objects that fell out of the 1:2 MMR and were subsequently trapped in other resonances. The dotted curve is the expected lower limit of the eccentricity as predicted by the adiabatic theory: $\sqrt{1/2} \log(a/a_{\text{edge}})$, where a is their current semi-major axis and a_{edge} is the primordial outer edge of the disk. So, if we place the original edge at, say, 30 AU, the expected eccentricity at 40 AU should be greater than 0.38. If this were true, we could not produce the cold population, which is between ~40 AU and 48 AU and has eccentricities less than ~0.2, with the adiabatic model. **c**, Our simulation in which the resonant particles are massive. The colours have the same meaning as in panel **b**. **d**, Our final simulation with massive disk particles and jumpy migration. The data were taken at 1 Gyr and only those particles with semi-major axes greater than 41 AU were plotted so as to keep it consistent with the definition of the cold belt.

there was indeed a population of low-inclination objects captured in Neptune's 1:2 resonance and pushed beyond the original outer edge of the disk, as predicted by the adiabatic theory.

In contrast with the theory, however, we found that some objects in the MMR have eccentricities that oscillate (Fig. 2) and thus there was always a population of bodies with small eccentricities (see Fig. 1c). These oscillations are the result of a previously unknown secular resonance that is embedded in Neptune's 1:2 MMR (Fig. 3). This secular resonance is generated when there is a significant amount of mass (~ 3 Earth masses) in the 1:2 MMR (see legend of Fig. 3).

How far can the bodies be pushed within the 1:2 MMR and still exhibit large eccentricity oscillations? Unfortunately, we cannot answer this with our current simulations for computational reasons. Because the amount of processing time required for our simulations is linear with respect to the number of disk particles, we were forced to keep the number of particles less than about 10^4 . In reality, the disk was made of many billions of much less massive objects. Consequently, Neptune's migration was much more jumpy in our simulation than it was in reality, which had the effect of artificially clearing objects from the 1:2 MMR (and other resonances) when it was at 38 AU, well before it entered the region of the cold Kuiper belt.

To overcome this problem, we performed a second simulation, in which planetary migration is not directly the result of the interaction with the disk particles, but instead is primarily induced by the inclusion of an artificial drag term in the planets' equations of motion. For this drag we employ the prescription in ref. 7, so that planetary migration is perfectly smooth and exponentially decreasing on a timescale of 40 Myr. The initial orbital configurations of the planets and particles in the 1:2 MMR are those obtained from the previous simulation when the resonance is exactly at the disk's edge. All other disk particles are discarded from the system. The initial total mass of the population in the 1:2 MMR is about three Earth masses. During the integration the disk particles responded to the planets, but not to each other. The planets responded to one another, the disk particles, and the drag force. We found that, throughout the migration process, there were always a number of objects in the 1:2 resonance that had small eccentricities (Fig. 1c). Investigations of the behaviour of these particles show that they are

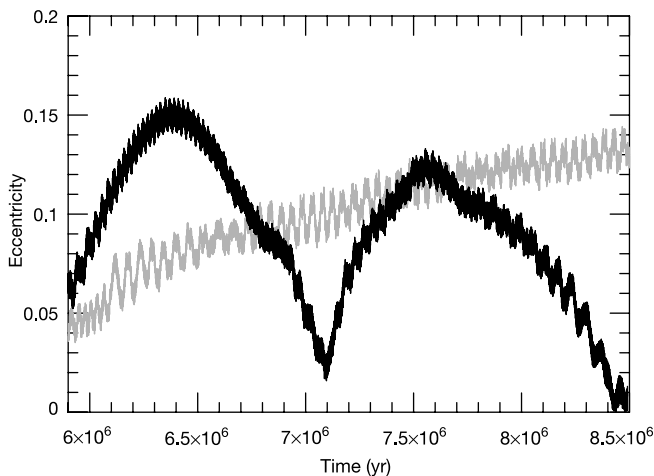


Figure 2 The evolution of eccentricity of particles in the 1:2 MMR in various physical situations. The black curve shows the eccentricity evolution of a resonant particle in our N -body integration after the resonance was pushed beyond the original disk edge (which occurred at $t = 5.9$ Myr). Large-amplitude secular oscillations temporarily drive the eccentricity down to $e \approx 0$. The grey curve shows the behaviour of a resonant particle's eccentricity when the population of massive 1:2 resonant bodies are replaced by an equal population of massless particles. In this case the overall eccentricity evolution is dominated by the monotonic growth, as predicted by the adiabatic theory. Therefore, the mass of the resonant population is the key to having a population of small-eccentricity objects as the 1:2 MMR sweeps through the region now occupied by the cold Kuiper belt.

indeed undergoing oscillations in eccentricity caused by the self-induced secular resonance described above.

So we were now able to produce resonant objects on low eccentricities as the resonance moved between 40 and 48 AU, but we still had not reproduced the observations. At the end of the simulation described in the previous paragraph, most of the objects are in the 1:2 resonance and not in the cold non-resonant population. Our model did not release enough of the objects from the resonance during the migration. This is because these simulations are the opposite extreme of our N -body simulations, that is, the migration is perfectly smooth. Perfectly smooth migration can only occur in an idealized disk composed of an infinite number of infinitely small objects.

In reality, Neptune's migration, and thus that of its MMRs, must have been somewhat jumpy because of the presence of relatively massive objects in the disk²⁵. Thus, we performed another simulation in which we modelled this by providing, at random times, instantaneous 'kicks' to Neptune's velocity in random directions. Figure 1d shows the resulting orbital distribution of the dynamically cold population produced in the simulation in which velocity kicks with magnitude $10^{-4}/\sqrt{p}$ km s⁻¹—where p was a uniform random number between 0 and 1—are applied every 5,000 years. The magnitude and frequency of these kicks statistically correspond to what Neptune would experience if there were one or two objects of about two lunar masses crossing its orbit at any one time. The $1/\sqrt{p}$ dependence is introduced to reproduce the statistical distribution of

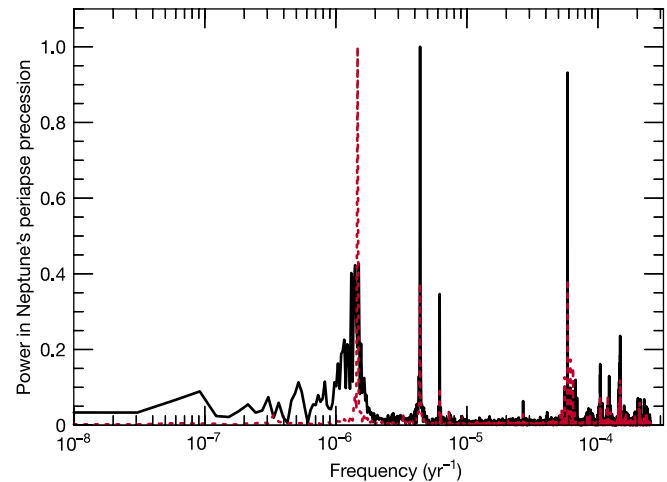


Figure 3 The power spectrum of the periape precession of Neptune's orbit that illustrates the origin of our new secular resonance. A secular resonance occurs when the body's longitude of perihelion precesses at the same rate as one of the frequencies of the planets. In a system consisting of only the four giant planets, the precession of Neptune's perihelion has four independent frequencies. The dotted red curve shows the frequency power spectrum of Neptune's longitude of perihelion in a planetary system where the semi-major axes of Jupiter, Saturn, Uranus and Neptune were at 5.5, 9.3, 15.4 and 22.0 AU, respectively. The slowest frequency is $\sim 1.5 \times 10^{-6}$ yr⁻¹, which is much faster than the precession frequencies of the perihelia of the bodies in the 1:2 MMR. Thus, no secular resonance occurs. However, when a non-negligible (about three Earth masses) amount of mass is placed in Neptune's 1:2 MMR, more frequencies are introduced into the power spectrum of Neptune's perihelion. If the mass were concentrated in one body only one new independent frequency would be introduced. But, if the mass is distributed among a population of objects with a variety of orbits and precession rates, Neptune's precession contains many more frequencies and many of these frequencies overlap, forming bands in the power spectrum. The solid black curve shows the case when we placed 780 particles, with a total of three Earth masses, in the resonance. Note that in this case the spectrum of Neptune exhibits frequencies of roughly 10^{-7} yr⁻¹, which are of the same order as the precession frequencies of the 1:2 MMR particles. Therefore, each body in the 1:2 resonance 'sees' a frequency in Neptune's motion that is close to its own, thereby causing a secular resonance. This situation forces large amplitude oscillations of the eccentricity, like those illustrated in Fig. 2.

impact parameters. There is reasonably good agreement between the observed orbital distribution of the cold population (Fig. 1a) and the results of our simulation. We also note that our new mechanism makes mainly cold objects—63% of the particles between 42 and 50 AU have inclinations less than 4° and all have inclinations less than ~15°.

We actually performed 12 ‘jumpy migration’ simulations with different values for the magnitude and frequency of the kicks. The run shown in Fig. 1d produced the semi-major axis versus eccentricity distribution most similar to that observed. Reducing the magnitude or the frequency of the kicks leaves progressively more particles in the 1:2 resonance at the end of the simulation, eventually conflicting with the observations. Conversely, increasing the magnitude or the frequency of the kicks leads to simulations where the resonance is depleted significantly before it reaches its final location and thus leaves no objects in the outer Kuiper belt, which again is in conflict with the observations.

The final cold belt population generated by our model represents only ~1% of the population originally in the massive planetesimal disk beyond the initial location of the 1:2 MMR. Obviously, this fraction is model-dependent, but it is necessarily small and explains the small mass of the current population. It is due to a series of successive diminutions related to: (1) the capture efficiency in the 1:2 MMR; (2) the probability of release from the resonance due to Neptune’s encounters with the massive bodies; and (3) the probability of having, at the time of the release from the resonance, an eccentricity sufficiently small to ensure survivability during the subsequent evolutionary phases.

The results presented in this Letter have profound implications for our understanding of the origin of the outer Solar System. In combination with the results in refs 6 and 7, this work implies that the entire Kuiper belt formed well within its current location, and achieved its present-day position as a result of Neptune’s outward migration. Unfortunately, the astronomical community does not, as yet, possess the computational ability to perform simulations of the entire process that include all three mechanisms. Therefore, whether this scheme can explain the ratio of the number of objects in the respective populations (resonant, cold and hot), the exact orbital elements of the Kuiper-belt objects, and the origin of the physical differences between the populations, must remain for future models to address.

However, even in its current form, our scheme does supply a natural explanation for the location of the Kuiper belt’s edge. Although several mechanisms have been proposed to explain the truncation of the proto-planetary disk^{14–17} (a requirement of our model), none can explain why it is near the location of Neptune’s 1:2 MMR. Our model explains this observation as a natural consequence of the dynamical evolution after the edge-forming event. Indeed, it predicts that although a few objects may eventually be discovered beyond the resonance on low-inclination, nearly circular orbits (because they can be formed by other dynamical mechanisms), they will be rare. Hence the Kuiper belt’s effective edge should be precisely at the current location of Neptune’s 1:2 MMR. □

Received 19 April; accepted 14 October 2003; doi:10.1038/nature02120.

1. Trujillo, C. A., Jewitt, D. C. & Luu, J. X. Properties of the Trans-Neptunian belt: statistics from the Canada-France-Hawaii telescope survey. *Astron. J.* **122**, 457–473 (2001).
2. Gladman, B. *et al.* The structure of the Kuiper belt: Size distribution and radial extent. *Astron. J.* **122**, 1051–1066 (2001).
3. Stern, S. A. & Colwell, J. E. Accretion in the Edgeworth-Kuiper belt: forming 100–1000 km radius bodies at 30 AU and beyond. *Astron. J.* **114**, 841–849 (1997).
4. Kenyon, S. J. & Luu, J. X. Accretion in the early Kuiper belt. I. Coagulation and velocity evolution. *Astron. J.* **115**, 2136–2160 (1998).
5. Morbidelli, A. & Brown, M. E. The Kuiper belt and the primordial evolution of the solar system. In *Comets II* (eds Festou, M., Keller, H. U. & Weaver, H.) (Univ. Arizona Press, Tucson, in the press).
6. Gomes, R. S. The origin of the Kuiper belt high inclination population. *Icarus* **161**, 404–418 (2003).
7. Malhotra, R. The origin of Pluto’s orbit: implications for the Solar System beyond Neptune. *Astron. J.* **110**, 420–432 (1995).
8. Jewitt, D. C. & Luu, J. X. Discovery of the candidate Kuiper belt object 1992 QB1. *Nature* **362**, 730–732 (1993).

9. Brown, M. The inclination distribution of the Kuiper belt. *Astron. J.* **121**, 2804–2814 (2001).
10. Levison, H. F. & Stern, S. A. On the size dependence of the inclination distribution of the main Kuiper belt. *Astron. J.* **121**, 1730–1735 (2001).
11. Trujillo, C. A. & Brown, M. E. A correlation between inclination and color in the classical Kuiper belt. *Astrophys. J.* **566**, 125–128 (2002).
12. Trujillo, C. A. & Brown, M. E. The radial distribution of the Kuiper belt. *Astrophys. J.* **554**, 95–98 (2001).
13. Allen, R. L., Bernstein, G. M. & Malhotra, R. Observational limits on a distant cold Kuiper belt. *Astron. J.* **124**, 2949–2954 (2002).
14. Ida, S., Larwood, J. & Burkert, A. Evidence for early stellar encounters in the orbital distribution of Edgeworth-Kuiper belt objects. *Astrophys. J.* **528**, 351–356 (2000).
15. Weidenschilling, S. Formation of planetesimals/cometesimals in the solar nebula. In *Comets II* (eds Festou, M., Keller, H. U. & Weaver, H.) (Univ. Arizona Press, Tucson, in the press).
16. Hollenbach, D. & Adams, F. C. Dispersal of disks around young stars: constraints on Kuiper belt formation. In *Debris Disks and the Formation of Planets* (eds Caroff, L. & Backman, D.) (ASP, San Francisco, in the press).
17. Stone, J. M., Gammie, C. F., Balbus, S. A. & Hawley, J. F. in *Protostars and Planets IV* (eds Mannings, V., Boss, A. P. & Russell, S. S.) 589–612 (Univ. Arizona Press, Tucson, 1998).
18. Fernández, J. A. & Ip, W. H. Orbital expansion and resonant trapping during the late accretion stages of the outer planets. *Planet. Space Sci.* **44**, 431–439 (1996).
19. Morbidelli, A. & Levison, H. F. Kuiper belt interlopers. *Nature* **422**, 30–31 (2003).
20. Duncan, M. & Levison, H. A scattered disk of icy objects and the origin of Jupiter-family comets. *Science* **276**, 1670–1672 (1997).
21. Luu, J. *et al.* A new dynamical class in the trans-Neptunian Solar System. *Nature* **387**, 573 (1997).
22. Gomes, R. S., Morbidelli, A. & Levison, H. F. Planetary migration in a planetesimal disk: why did Neptune stop at 30 AU? *Icarus* (submitted).
23. Duncan, M. J., Levison, H. F. & Lee, M.-H. A multiple timestep symplectic algorithm for integrating close encounters. *Astron. J.* **116**, 2067–2077 (1998).
24. Wisdom, J. & Holman, M. Symplectic maps for the n-body problem. *Astron. J.* **102**, 1528–1538 (1991).
25. Hahn, J. M. & Malhotra, R. Orbital evolution of planets embedded in a planetesimal disk. *Astron. J.* **117**, 3041–3053 (1999).

Acknowledgements We are grateful to R. Gomes and M. Holman for acting as referees on this paper. We also thank L. Dones, W. Bottke, J.-M. Petit, and K. Tsiganis for help with an early version of the text and M. Duncan and R. Gomes for discussions. H.F.L. is grateful for funding from NASA. We thank the CNRS and NSF for encouraging friendly relationships between the US and France.

Competing interests statement The authors declare that they have no competing financial interests.

Correspondence and requests for materials should be sent to H.F.L. (hal@boulder.swri.edu).

Microfluidic sorting in an optical lattice

M. P. MacDonald¹, G. C. Spalding^{1,2} & K. Dholakia¹

¹School of Physics and Astronomy, University of St Andrews, North Haugh, St Andrews, Fife KY16 9SS, UK

²Department of Physics, Illinois Wesleyan University, Bloomington, Illinois 61702, USA

The response of a microscopic dielectric object to an applied light field can profoundly affect its kinetic motion¹. A classic example of this is an optical trap, which can hold a particle in a tightly focused light beam². Optical fields can also be used to arrange, guide or deflect particles in appropriate light-field geometries^{3,4}. Here we demonstrate an optical sorter for microscopic particles that exploits the interaction of particles—biological or otherwise—with an extended, interlinked, dynamically reconfigurable, three-dimensional optical lattice. The strength of this interaction with the lattice sites depends on the optical polarizability of the particles, giving tunable selection criteria. We demonstrate both sorting by size (of protein microcapsule drug delivery agents) and sorting by refractive index (of other colloidal particle streams). The sorting efficiency of this method approaches 100%, with values of 96% or more observed even for concentrated solutions with throughputs exceeding those reported for fluorescence-activated cell sorting⁵. This powerful, non-invasive technique is suited to sorting and fractionation within integrated